

## Flavour anomalies versus high- $p_T$ physics

A. GRELJO (\*)

*Physik-Institut, Universität Zürich, CH-8057 Zürich, Switzerland*

### Summary. —

I discuss the implications of the long-standing anomaly in semi-tauonic  $B$  meson decays for new physics (NP) searches at high- $p_T$  with ATLAS and CMS detectors. Effective field theory is used to identify potential signatures at high energies correlated with the anomaly. Several representative models put forward to explain the anomaly are examined in details: color-neutral vector triplet, 2HDM, scalar and vector leptoquark model. We find that in general  $\tau^+\tau^-$  searches impose serious challenge to NP explanations of the anomaly. After recasting present 8 and 13 TeV analyses stringent limits are set on all the models.

PACS 13.20.He

### 1. – Hints on Lepton Flavour Non-Universality in charged currents

Over the past several years, there has been accumulating evidence for departures from Lepton Flavour Universality (LFU) in (semi)tauonic decays of  $B$  mesons. In particular, all reported measurements of LFU ratios

$$(1) \quad R(D^{(*)}) \equiv \frac{\Gamma(B \rightarrow D^{(*)}\tau\nu)}{\Gamma(B \rightarrow D^{(*)}\ell\nu)},$$

where  $\ell = e, \mu$ , are systematically larger than the corresponding SM predictions. A recent HFAG average of all current measurements [1]

$$(2) \quad R(D^*) = (1.25 \pm 0.07) \times R(D^*)_{\text{SM}},$$

$$(3) \quad R(D) = (1.32 \pm 0.16) \times R(D)_{\text{SM}},$$

---

(\*) I would like to thank my collaborators: Dario Buttazzo, Darius A. Faroughy, Gino Isidori, Jernej F. Kamenik and David Marzocca.

puts the combined significance of these excesses at the  $4.0\sigma$  level. Both  $R(D^{(*)})$  exhibit deviations of the same order and a good fit to current data prefers an approximately universal enhancement of  $\sim 30\%$  in both observables over their SM values. This relatively large effect in charged current mediated weak processes calls for new physics (NP) contributions in  $b \rightarrow c\tau\nu$  transitions. At the tree level, the possibilities are reduced to the exchange of a charged scalar ( $H^+$ ) or vector ( $W'$ ) bosons, or alternatively colored states carrying baryon and lepton numbers (leptoquarks). Importantly, all possibilities imply new charged (and possibly colored) states with masses at or below the TeV and with significant couplings to the third generation SM fermions, making them potential targets for direct searches at the LHC. In particular, I will show that quite generally NP relevant to the  $R(D^{(*)})$  anomalies can be efficiently probed using high- $p_T$  tau pair production at the LHC [2, 3, 4]. This talk is based mainly on the Ref. [2].

## 2. – Correlated signal at the high- $p_T$ — General discussion

**2.1.  $SU(2)_L$  prediction: Neutral currents.** – While the effects in (semi)leptonic  $B$  decays can without loss of generality be described in terms of effective operators respecting the QCD and QED gauge symmetries relevant below the electroweak breaking scale, this is certainly not suitable for processes occurring at LHC energies. To fully explore the possible high- $p_T$  signatures associated with effects in  $R(D^{(*)})$ , a set of semileptonic dimension six operators invariant under the full SM gauge symmetry is required. In the following we adopt the complete basis

$$\begin{aligned} \mathcal{L}^{\text{eff}} \supset & c_{QQLL}^{ijkl} (\bar{Q}_i \gamma_\mu \sigma^a Q_j) (\bar{L}_k \gamma^\mu \sigma_a L_l) \\ & + c_{QuLe}^{ijkl} (\bar{Q}_i u_R^j) i\sigma^2 (\bar{L}_k \ell_R^l) + c_{dQLe}^{ijkl} (\bar{d}_R^i Q_j) (\bar{L}_k \ell_R^l) \\ & + c_{QuLe'}^{ijkl} (\bar{Q} \sigma_{\mu\nu} u_R^j) i\sigma^2 (\bar{L} \sigma^{\mu\nu} \ell_R^l) + \text{h.c.}, \end{aligned} \quad (4)$$

where  $Q_i = (V_{ji}^* u_L^j, d_L^i)^T$  and  $L_i = (U_{ji}^* \nu^j, \ell_L^i)^T$  are the SM quark and lepton weak doublets in a basis which coincides with the mass-ordered mass-eigenbasis of down-like quarks ( $d^i$ ) and charged leptons ( $\ell^i$ ),  $V(U)$  is the CKM (PMNS) flavor mixing matrix and  $\sigma^a$  are the Pauli matrices acting on  $SU(2)_L$  indices (suppressed).

First observation that can be made at this point is that in addition to charged current ( $u^i \rightarrow d^j \ell^k \nu^l$ ) transitions, all operators predict the appearance of neutral quark and lepton currents ( $u^i \bar{u}^j \rightarrow \ell^k \bar{\ell}^l$  and/or  $d^i \bar{d}^j \rightarrow \ell^k \bar{\ell}^l$ ). To proceed further, we need to specify the flavor structure of the operators. We work with a particular choice of flavor alignment (consistent with an  $U(2)$  flavor symmetry acting on the first two generations of SM fermions), namely  $c_{QQLL}^{ijkl} \simeq c_{QQLL} \delta_{i3} \delta_{j3} \delta_{k3} \delta_{l3}$ ,  $c_{dQLe}^{ijkl} \simeq c_{dQLe} \delta_{i3} \delta_{j3} \delta_{k3} \delta_{l3}$ , which is motivated by (1) the requirement that the dominant effects appear in charged currents coupling to  $b$ -quarks and tau-leptons, and (2) stringent constraints on flavor changing neutral currents (FCNCs). Small deviations from this limit, consistent with existing flavor constraints, would however not affect our conclusions. A common and crucial consequence of these flavor structures is that  $b \rightarrow c$  quark currents always carry additional flavor suppression of the order  $\sim |V_{cb}| \simeq 0.04$  compared to the dominant  $b \rightarrow t$  (charged current) and  $b \rightarrow b$ ,  $t \rightarrow t$  (neutral current) transitions.

We are now in a position to identify the relevant LHC signatures at high- $p_T$ . The main focus of this work is on  $\tau^+ \tau^-$  production from heavy flavor annihilation in the colliding protons ( $b \bar{b} \rightarrow \tau^+ \tau^-$ ). Even though it is suppressed by small heavy quark PDF,

this signature is extremely constraining for a particular explicit NP model addressing the  $R(D^{(*)})$  anomaly, owing in particular to the  $\sim 1/|V_{cb}|$  enhancement of the relevant  $b\bar{b} \rightarrow \tau^+\tau^-$  neutral current process over the charged  $b \rightarrow c\tau\nu$  transition, as dictated by flavor constraints. As discussed above, in the EW preserving limit and in absence of cancelations a similar conclusion can be reached individually for terms in Eq. 4 proportional to  $c_{QQLL}$  and  $c_{dQLe}$  but not the ones proportional to  $c_{QuLe}$  and  $c_{QuLe'}$ . Obviously, no such flavor enhancement is there for the related charged current mediated process of  $\tau^+\nu$  production from  $\bar{b}c$  annihilation. The resulting constraints thus turn out not to be competitive.

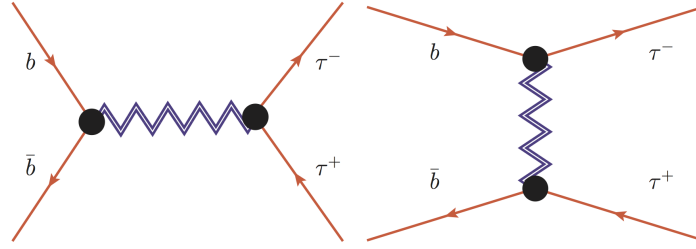


Fig. 1. – Diagrammatic representation of  $s$ -channel (left-hand side) and  $t$ -channel (right-hand side) resonance exchange (drawn in blue double see-saw lines) contributions to  $b\bar{b} \rightarrow \tau^+\tau^-$  process.

**2.2. Single mediator models: Signatures.** – The different chiral structures being probed by  $R(D^{(*)})$  single out a handful of simplified single mediator models. In the following we consider the representative cases, where we extend the SM by a single field transforming non-trivially under the SM gauge group.

First categorization of single mediators is by color. While colorless intermediate states can only contribute to  $b \rightarrow c\tau\nu$  transitions in the  $s \equiv (p_b - p_c)^2$ -channel, colored ones can be exchanged in the  $t \equiv (p_b - p_\tau)^2$ - or  $u \equiv (p_b - p_\nu)^2$ -channels. The colorless fields thus need to appear in non-trivial  $SU(2)_L$  multiplets (doublets or triplets) where the charged state mediating semileptonic charged currents is accompanied by one or more neutral states mediating neutral currents. Such models thus predict  $\hat{s} \equiv (p_{\tau^+} + p_{\tau^-})^2$ -channel resonances in  $\tau^+\tau^-$  production (see the left-hand side diagram in Fig. 1). In addition to the relevant heavy quark and tau-lepton couplings, searches based on the on-shell production of these resonances depend crucially on the assumed width of the resonance. Alternatively, colored mediators (leptoquarks) can be  $SU(2)_L$  singlets, doublets or triplets, carrying baryon and lepton numbers. Consequently they will again mediate  $\tau^+\tau^-$  production, this time through  $\hat{t} \equiv (p_b - p_{\tau^-})^2$ - or  $\hat{u} \equiv (p_b - p_{\tau^+})^2$ -channel exchange (see the right-hand side diagram in Fig. 1). In this case a resonant enhancement of the high- $p_T$  signal is absent, however, the searches do not (crucially) depend on the assumed width (or equivalently possible other decay channels) of the mediators.

### 3. – Di-tau searches at the LHC

The exclusion limits presented below are based on the reinterpretation of the ATLAS analyses in Refs. [6, 7, 8]. Specifically, we have performed a recast of the 8 TeV and 13 TeV inclusive search for a neutral  $Z'$  in the  $\tau_{\text{had}}\tau_{\text{had}}$  channel. This recast sets exclusion limits on high-mass resonances in the range 0.5–2.5 TeV but is less sensitive to resonances

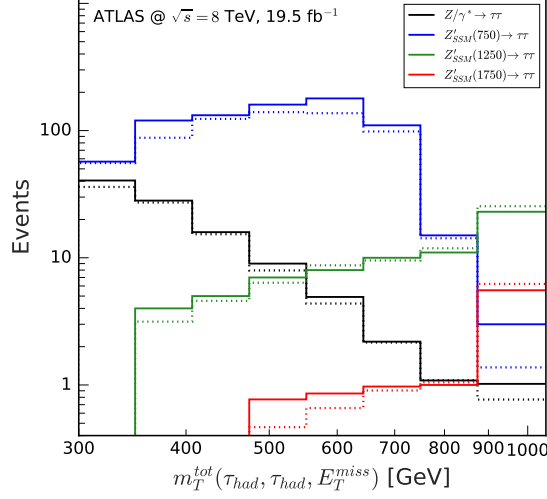


Fig. 2. – Simulation procedure validation plot. Solid (dashed) are predictions for the SM background and sequential  $Z'$  models from ATLAS (our simulation).

with masses below 500 GeV. In order to cover the low-mass region we performed a recast of a recent 13 TeV MSSM neutral Higgs search with  $13.2 \text{ fb}^{-1}$  in the  $\tau_{\text{had}}\tau_{\text{had}}$  channel. This last search is more sensitive to resonances in the mass range  $0.2 - 1.2 \text{ TeV}$  because of better statistics due to higher luminosity.

For the collider simulations, we have implemented the EFT and the simplified models discussed here with the Universal File Output (UFO) format generated by **FeynRules 2**. For each model we generated with **Madgraph 5** large samples of  $pp(b\bar{b}) \rightarrow \tau^+\tau^-$  events at LO. Both **Pythia 6** and **Pythia 8.210** were used to decay the  $\tau$ -leptons, simulate parton showering and include hadronization. Any effects due to spin correlations for the  $\tau$ -decays were neglected. The detector response was simulated with **Delphes 3** coupled with **FastJet** for jet clustering. The ATLAS Delphes card was modified to satisfy the object reconstruction and identification requirements used in each of the experimental searches, in particular the corresponding  $\tau_{\text{had}}$ -tagging and  $b$ -tagging efficiencies were set accordingly.

Following the  $Z'$  search, events were selected if they contained at least two identified  $\tau_{\text{had}}$ , one with  $p_T > 150 \text{ GeV}$  [6] ( $p_T > 110 \text{ GeV}$  [7]) and the other with  $p_T > 50 \text{ GeV}$  [6] ( $p_T > 55 \text{ GeV}$  [7]), no electrons with  $p_T > 15 \text{ GeV}$ , and no muons with  $p_T > 10 \text{ GeV}$ . Additionally, the visible part of the candidate  $\tau_{\text{had}}\tau_{\text{had}}$  pair had to be of opposite-sign (OS) and produced back-to-back in the azimuthal plane with  $\Delta\phi(\tau_1, \tau_2) > 2.7 \text{ rad}$ . Finally, in order to reconstruct the mass of the  $\tau_{\text{had}}\tau_{\text{had}}$  pair, the selected events were binned into signal regions defined by different threshold values of the total transverse mass  $m_T^{\text{tot}}$ . Here the total transverse mass  $m_T^{\text{tot}}$  of the visible part of  $\tau_{\text{had}}\tau_{\text{had}}$  is defined by

$$(5) \quad m_T^{\text{tot}} \equiv \sqrt{m_T^2(\tau_1, \tau_2) + m_T^2(\cancel{E}_T, \tau_1) + m_T^2(\cancel{E}_T, \tau_2)},$$

where  $m_T(A, B) = \sqrt{p_T(A)p_T(B)[1 - \cos\Delta\phi(A, B)]}$  is the transverse mass between objects  $A$  and  $B$ , and  $\cancel{E}_T$  is the total missing transverse energy reconstructed in the event.

For the recast of Ref. [6] we used the  $m_T^{\text{tot}}$  thresholds, observed data and expected background events from Table 4 in [6]. For the recast of Ref. [7], the thresholds  $m_T^{\text{tot}} > 150, 186, 231, 287, 357, 444, 551$  and  $684$  GeV and other quantities were directly extracted from Fig. 4(f) in [7]. Our simulations and event selections were carefully validated by comparing our results with those obtained by ATLAS in [6, 7] for both background and signal Drell-Yan samples  $pp \rightarrow \tau_{\text{had}}\tau_{\text{had}}$  mediated by  $Z/\gamma^*$  in the SM and by  $Z'$  in the SSM as shown in Fig. 2.

#### 4. – Single mediator model examples — Exclusion limits

**4.1.  $W'$  model.** – A color-neutral real  $SU(2)_L$  triplet of massive vectors  $W'^a \sim W'^{\pm}, Z'$  can be coupled to the SM fermions via

$$(6) \quad \begin{aligned} \mathcal{L}_{W'} &= -\frac{1}{4}W'^{a\mu\nu}W'_{\mu\nu} + \frac{M_{W'}^2}{2}W'^{a\mu}W'_\mu + W'_\mu J_{W'}^{a\mu} , \\ J_{W'}^{a\mu} &\equiv \lambda_{ij}^q \bar{Q}_i \gamma^\mu \sigma^a Q_j + \lambda_{ij}^\ell \bar{L}_i \gamma^\mu \sigma^a L_j . \end{aligned}$$

Since the largest effects should involve  $B$ -mesons and tau leptons we assume  $\lambda_{ij}^{q(\ell)} \simeq g_{b(\tau)} \delta_{i3} \delta_{j3}$ , consistent with an  $U(2)$  flavor symmetry [3]. Departures from this limit in the quark sector are constrained by low energy flavor data, including meson mixing, rare  $B$  decays, LFU and LFV in  $\tau$  decays and neutrino physics, a detail analysis of which has been performed in Ref. [3]. The main implication is that the LHC phenomenology of heavy vectors is predominantly determined by their couplings to the third generation fermions ( $g_b$  and  $g_\tau$ ).

In addition, electroweak precision data require  $W'$  and  $Z'$  components of  $W'^a$  to be degenerate up to  $\mathcal{O}(\%)$ , with two important implications: (1) it allows to correlate NP in charged currents at low energies and neutral resonance searches at high- $p_T$ ; (2) the robust LEP bounds on pair production of charged bosons decaying to  $\tau\nu$  final states can be used to constrain the  $W'$  mass from below  $\sim 100$  GeV. Finally,  $W'^a$  coupling to the Higgs current ( $W'_a H^\dagger \overset{\leftrightarrow}{D}_\mu H$ ) needs to be suppressed, and thus irrelevant for the phenomenological discussions at the LHC.

Integrating out heavy  $W'^a$  at tree level, generates the four-fermion operator,

$$(7) \quad \mathcal{L}_{W'}^{\text{eff}} = -\frac{1}{2M_{W'}^2} J_{W'}^{a\mu} J_{W'}^{a\mu} ,$$

and after expanding  $SU(2)_L$  indices,

$$(8) \quad \begin{aligned} \mathcal{L}_{W'}^{\text{eff}} &\supset -\frac{\lambda_{ij}^q \lambda_{kl}^\ell}{M_{W'}^2} (\bar{Q}_i \gamma_\mu \sigma^a Q_j) (\bar{L}_k \gamma^\mu \sigma^a L_l) \\ &\supset -\frac{g_b g_\tau}{M_{W'}^2} (2V_{cb} \bar{c}_L \gamma^\mu b_L \bar{\tau}_L \gamma_\mu \nu_L + \bar{b}_L \gamma^\mu b_L \bar{\tau}_L \gamma_\mu \tau_L) . \end{aligned}$$

The resolution of the  $R(D^{(*)})$  anomaly requires  $c_{QQLL} \equiv -g_b g_\tau / M_{W'}^2 \simeq -(2.1 \pm 0.5) \text{ TeV}^{-2}$ , leading at the same time to potentially large  $b \bar{b} \rightarrow Z' \rightarrow \tau^+ \tau^-$  signal at the LHC. Here we recast existing LHC  $\tau\tau$  searches including possible large resonance width effects in order to properly extract the LHC limits on this model.

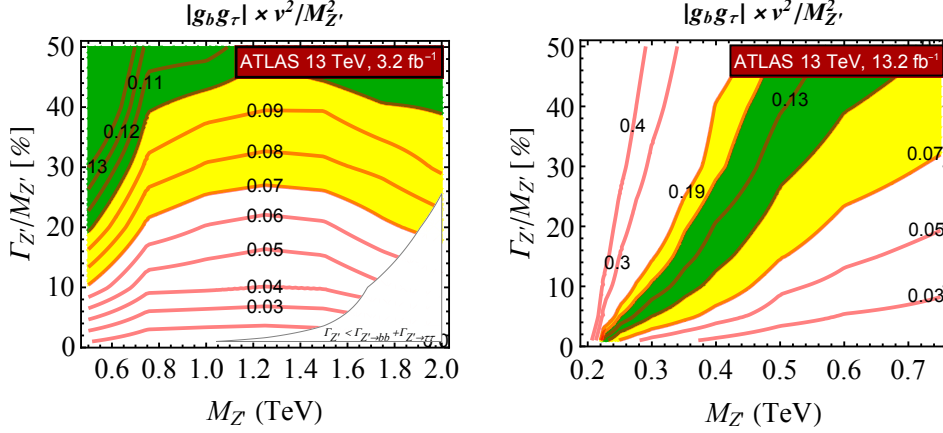


Fig. 3. – Recast of ATLAS  $\tau^+\tau^-$  searches at 13 TeV with  $3.2 \text{ fb}^{-1}$  [7] (left plot) and  $13.2 \text{ fb}^{-1}$  [8] (right plot) as exclusion limits on the  $b\bar{b}$  induced spin-1  $\tau^+\tau^-$  resonance ( $b\bar{b} \rightarrow Z' \rightarrow \tau\tau$ ). Isolines shown in red represent upper limits on the combination  $|g_b g_\tau| \times v^2 / M_{Z'}^2$ , as a function of the  $Z'$  mass and total width. The  $R(D^{(*)})$  preferred regions  $|g_b g_\tau| \times v^2 / M_{Z'}^2 = (0.13 \pm 0.03)$  at 68% and 95% CL are shaded in green and yellow, respectively.

The resulting 95% CL upper limits on the  $|g_b g_\tau| \times v^2 / M_{Z'}^2$ , for a given  $Z'$  mass and total decay width, after recasting ATLAS search at 13 TeV with  $3.2 \text{ fb}^{-1}$  [7] (left plot) and 13 TeV with  $13.2 \text{ fb}^{-1}$  [8] (right plot)  $\tau^+\tau^-$  searches, respectively, are shown in Fig. 3 and marked with red isolines. Note that this way of presenting results is independent of the assumption on the existence of extra  $Z'$  decay channels. The white region with gray border is not constrained since the assumed total width there is smaller than the minimum possible sum of the partial widths to  $b\bar{b}$  and  $\tau^+\tau^-$  computed at the current experimental upper bound on  $|g_b g_\tau| / M_{Z'}^2$ . These exclusions are to be compared with the preferred value from the fit to the  $R(D^{(*)})$  anomaly,  $|g_b g_\tau| \times v^2 / M_{Z'}^2 = (0.13 \pm 0.03)$ , indicated in green ( $1\sigma$ ) and yellow ( $2\sigma$ ) shaded regions in the plot.

To conclude, for relatively heavy vectors  $M_{W'} > 500 \text{ GeV}$  within the vector triplet model, the resolution of the  $R(D^{(*)})$  anomaly and consistency with existing  $\tau^+\tau^-$  resonance searches at the LHC require a very large  $Z'$  total decay width. Perturbative calculations arguably fail in this regime. In other words, within the weakly coupled regime of this setup the resolution of the  $R(D^{(*)})$  anomalies cannot be reconciled with the existing LHC  $\tau^+\tau^-$  searches. On the other hand, interestingly, a light  $Z'$  resonance with  $M_{Z'} < 400 \text{ GeV}$ , a relatively small width and couplings compatible with the  $W'$  resolution of the  $R(D^{(*)})$  anomaly is not excluded by our  $\tau^+\tau^-$  search recast.

**4.2. Vector  $LQ$  model.** – One can also extend the SM with a vector leptoquark weak singlet,  $U_\mu \equiv (\mathbf{3}, \mathbf{1}, 2/3)$ , coupled to the left-handed quark and lepton currents,

$$\begin{aligned} \mathcal{L}_U = & -\frac{1}{2} U_{\mu\nu}^\dagger U^{\mu\nu} + M_U^2 U_\mu^\dagger U^\mu + (J_U^\mu U_\mu + \text{h.c.}) , \\ (9) \quad J_U^\mu \equiv & \beta_{ij} \bar{Q}_i \gamma^\mu L_j , \end{aligned}$$

where again we restrict our discussion to  $\beta_{ij} \simeq g_U \delta_{3i} \delta_{3j}$ , consistent with a  $U(2)$  flavor symmetry [5]. Low energy flavor phenomenology of such models implies that the third

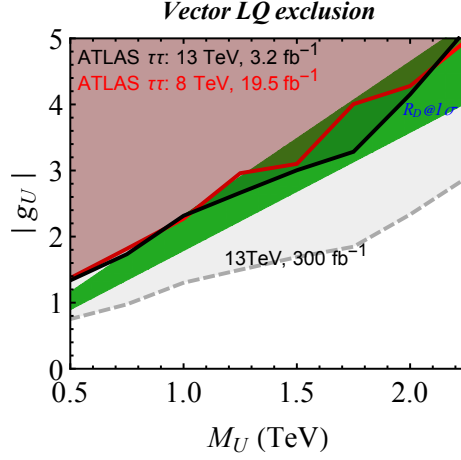


Fig. 4. – ATLAS 8 TeV [6] (13 TeV [7])  $\tau^+\tau^-$  search exclusion limits are shown in red (black) and  $R(D^{(*)})$  preferred region in green for the vector leptoquark model. Projected 13 TeV limits for  $300 \text{ fb}^{-1}$  are shown in grey.

generation fermion couplings dominate the phenomenological discussion also at the LHC.

Unlike in the case of colorless mediators, QCD induced leptoquark pair production can lead to a large signal rate at the LHC, thus yielding robust constraints on the leptoquark mass  $M_U$ . In the exact  $U(2)$  flavor limit,  $\mathcal{B}(U \rightarrow t\nu) = \mathcal{B}(U \rightarrow b\tau) = 0.5$ . Revisiting the ATLAS search for QCD pair-produced third generation scalar leptoquark in the  $t\bar{t}\nu\bar{\nu}$  channel, Ref. [5] excludes  $M_U < 770 \text{ GeV}$ .

Integrating out the heavy  $U_\mu$  field at the tree level, the following effective dimension six interaction is generated

$$(10) \quad \mathcal{L}_U^{\text{eff}} = -\frac{1}{M_U^2} J_U^{\mu\dagger} J_U^\mu .$$

Using Fierz identities to match the above expression onto the operator basis in Eq. 4, one finds

$$(11) \quad \mathcal{L}_U^{\text{eff}} = -\frac{\beta_{il}\beta_{kj}^\dagger}{2M_U^2} [(\bar{Q}_i\gamma_\mu\sigma^a Q_j)(\bar{L}_k\gamma^\mu\sigma_a L_l) + (\bar{Q}_i\gamma_\mu Q_j)(\bar{L}_k\gamma^\mu L_l)] ,$$

which finally leads to

$$(12) \quad \mathcal{L}_U^{\text{eff}} \supset -\frac{|g_U|^2}{M_U^2} [V_{cb}(\bar{c}_L\gamma^\mu b_L)(\bar{\tau}_L\gamma_\mu \nu_L) + (\bar{b}_L\gamma^\mu b_L)(\bar{\tau}_L\gamma_\mu \tau_L)] .$$

The fit to  $R(D^{(*)})$  anomaly requires  $|g_U|^2/M_U^2 \equiv 2|c_{QQLL}| \simeq (4.3 \pm 1.0) \text{ TeV}^{-2}$ . As a consequence, sizeable  $b\bar{b} \rightarrow \tau^+\tau^-$  signal at LHC is induced via t-channel vector LQ exchange.

The  $\tau^+\tau^-$  production through t-channel leptoquark exchange is only known at LO in QCD and we simulate it using the NNPDF2.3 PDF set at NLO in the 5-flavor scheme. The exclusion limits for the vector leptoquark model from the recast of 8 TeV [6] and 13 TeV [7] searches are shown in Fig. 4 (top) in red and black shades, respectively. On the other hand, the preferred region at 68% CL from  $R(D^{(*)})$  anomaly is shown in green.

In addition, projected exclusion limits at 13 TeV, with  $300 \text{ fb}^{-1}$  (assuming the present 13 TeV limits on the cross-section to scale with the square root of the luminosity ratio) are shown in gray. In this model, the  $R(D^{(*)})$  anomaly explanation is already in some tension with existing  $\tau^+\tau^-$  searches, and future LHC Run-II data should resolve the issue conclusively.

## 5. – Conclusions

I discussed in this talk possible new dynamics that could explain the recent hints of LFU violation in (semi)tauonic  $B$  meson decays, and, in particular, *the physics case* for associated high- $p_T$  searches at the LHC [2]. By employing effective field theory methods we have argued that in presence of non-standard effects in semi-leptonic charged currents, one in general expects signals also in neutral currents involving charged leptons. Moreover, requiring (i) dominant couplings to the third generation in order to explain the  $R(D^{(*)})$  anomaly and (ii) protection from large FCNC in the down quark sector, neutral currents involving pure third generation fermions ( $bb \rightarrow \tau\tau$ ) are  $\sim 1/V_{cb}$  enhanced with respect to  $bc \rightarrow \tau\nu$  charged currents, leading to potentially large signals at the LHC.

Indeed, by performing a recast of existing  $\tau^+\tau^-$  resonance searches at the LHC, we set stringent limits on several representative simplified models involving: a spin-1 colorless weak triplet, a 2HDM, a spin-0 or spin-1 leptoquark. We find that in light of existing constraints it is paramount to consider (relatively) wide and (or) light resonances, and we encourage the experimental collaborations to perform and update their searches for  $\tau^+\tau^-$  resonances in a model independent way as illustrated in Fig. 3. At the same time, searches for non-resonant deviations in (the tails of) distributions are equally relevant as shown in the leptoquark analysis (see Fig. 4).

Possibilities within more elaborate new physics models to avoid the current stringent constraints include (i) splitting the neutral and charged states in the weak multiplet or (ii) providing additional negatively interfering contributions in  $\tau^+\tau^-$  production, both of which require a degree of fine tuning.

\* \* \*

This work is supported in part by the Swiss National Science Foundation (SNF) under contract 200021-159720.

## REFERENCES

- [1] Y. Amhis *et al.* [Heavy Flavor Averaging Group (HFAG) Collaboration], arXiv:1412.7515 [hep-ex] and online update at <http://www.slac.stanford.edu/xorg/hfag>.
- [2] D. A. Faroughy, A. Greljo and J. F. Kamenik, Phys. Lett. B **764** (2017) 126 doi:10.1016/j.physletb.2016.11.011 [arXiv:1609.07138 [hep-ph]].
- [3] A. Greljo, G. Isidori and D. Marzocca, JHEP **1507** (2015) 142 doi:10.1007/JHEP07(2015)142 [arXiv:1506.01705 [hep-ph]].
- [4] D. Buttazzo, A. Greljo, G. Isidori and D. Marzocca, JHEP **1608** (2016) 035 doi:10.1007/JHEP08(2016)035 [arXiv:1604.03940 [hep-ph]].
- [5] R. Barbieri, G. Isidori, A. Pattori and F. Senia, Eur. Phys. J. C **76** (2016) no.2, 67 doi:10.1140/epjc/s10052-016-3905-3 [arXiv:1512.01560 [hep-ph]].
- [6] G. Aad *et al.* [ATLAS Collaboration], JHEP **1507** (2015) 157 doi:10.1007/JHEP07(2015)157 [arXiv:1502.07177 [hep-ex]].
- [7] The ATLAS collaboration, CERN-EP-2016-164. [arXiv:1608.00890v2 [hep-ex]]
- [8] The ATLAS collaboration, ATLAS-CONF-2016-085.